

- A low corrosion resistance was observed for the materials in whose hardening products highly basic hydrosilicates, portlandite, iron oxides and hydroxides dominate.
- A different situation was observed when silica-containing additives were added to Portland cement. These additives were represented by quartz sand (Portland cement 60% + barite 40% + sand 30%) or by milled clinoptolite (Portland cement 70% + zeolite 30%). Such specimens sustained tests indicating high gas impermeability.
- 20% ash of burnable slates with high calcium content was introduced into the cement-sand mixture. This test failed, corrosion resistance of this composition was low.
- The use of weighting additives with high content of iron oxides and hydroxides is not recommended.
- Hydrogen-sulfide resistance of Portland cement can be achieved by introducing silica-containing additives (quartz sand, zeolites), provided that they are highly dispersed giving rise to a sufficient reactivity of silica in a particular temperature range.

Slightly different but using the same components for a corrosion resistance property, some cement dust from electrostatic filters of cement plants is used as corrosion inhibitor protecting steel articles and constructions from effects of petroleum oil and strongly mineralized stratal waters, oil-water emulsions, H<sub>2</sub>S and CO<sub>2</sub> containing gases (Ivashov 1993). The dust contains (in wt.%):

- CaO: 44.0 - 48.0
- SiO<sub>2</sub>: 14.58 - 15.80
- Al<sub>2</sub>O<sub>3</sub>: 2.84 - 3.6
- Fe<sub>2</sub>O<sub>3</sub>: 2.66 - 3.29
- MgO: 1.0 - 1.86
- K<sub>2</sub>O: 1.7 - 2.36
- Na<sub>2</sub>O: 0.34 - 0.55

The dust also contains 0.5 - 5 g Ag/ton. It is used in dry form or in solution containing 0.3 - 0.6 g/l at pH 10-11.

#### 2.4 Addition of Silica in the Portland cement for an anti-corrosion effect

A general requirement for the use of Portland cement at the high temperatures associated with geothermal wells is the addition of silica, SiO<sub>2</sub>. This silica addition is typically in the form of a finely ground quartz silica, referred as silica flour. The purpose of this additional silica is to decrease the cement's CaO to SiO<sub>2</sub> (C/S) ratio and thereby stabilize the cement system at higher temperatures and prevent strength retrogression (Weber et. al. 1998).

Presence of carbon dioxide in a geothermal environment complicates the chemistry in formulating an acceptable Portland cement system. We have seen in the previous

paragraph that CO<sub>2</sub> induced chemical reactions result in the loss of cementitious material for the cement matrix resulting in increasing permeability and decreasing compressive strength. Some studies (Weber et. al. 1998) have indicated that the addition of silica for prevention of strength retrogression is at odds with the prevention of carbonation.

Yao and Liao et. al. (1998, 1996) state that by improving the permeability of the cement and reducing the content of Ca(OH)<sub>2</sub> in the cement, anticorrosion effects can be improved. Addition of silica flour changes the proportion of calcium and silica, and composition of hydrates. The proportion of silica flour is an essential aspect of the procedure. Experiments made at the Southwest Petroleum Institute in China (Yao 1998) show that when the temperature is inferior to 110°C, 5 to 8 % of silica flour should be added to the cement in order to increase the slurry density. When the temperature is superior to 110°C, 10 to 15 % of silica flour should be added. The same experimentations state that too much silica sand (35%) will give the opposite results, and therefore will yield to an increase of corrosion.

## **2.5 RPC, a Reactive Powders Cement**

The Institut Français du Pétrole has developed a Reactive Powders Cement formulation, RPC, for oil well cementation with enhanced mechanical properties (Noik et. al.).

### **2.5.1 Materials**

This material has been optimized while considering only the clinker composition and water content. The main idea was to manage with the mean particle size of each powder i.e. cement – sand – silica fume. Then, the rheological properties of this cement blend were optimized with dispersant and water contents. The amount of water (dispersant W/C = 0.27) was less than the classical W/C ratio of 0.44 for a conventional 1.9 g/cm<sup>3</sup> specific density slurry. So, the setting material was under saturated and still contained some reactive powders such as calcium silicate or silicate fume grains.

Classical materials such as Portland cement class G, crushed sand and silica fume were used. Additives such as fluid loss reducer, retarder and dispersant are organic products. They are respectively acrylic polymer, lignosulfonate derivative and polynaphthalene sulfonate. The weighting agents selected are hematite and manganese oxide particles.

### **2.5.2 Mixing procedure**

Powders and water were mixed in a blender at high-speed rate. Additives were previously diluted before in water.

### **2.5.3 Durability tests**

RPC formulation presented high compressive strength value, above 100 MPa, with very low permeability (1.2 E-7 mDa at 180°C) and maintained this performance over nearly one year.

The long-term behavior of RPC formulation was studied at 120°C, 140°C and 180°C. The variation over time of the compressive strength is represented in Table 2.1.

*Table 2.1: Durability at 120°C, 140°C and 180°C, compressive strength variation with RPC slurry*

Time	Compressive strength variation (MPa)		
	120°C	140°C	180°C
0 days	-	138.5	152
15 days	115	-	-
30 days	125	195	147.8
60 days	-	167.5	-
90 days	88.5	187.5	127
180 days	135	189	117.4
360 days	155	-	-

At 120°C and 140°C, an increase of the mechanical properties was observed over long period. At 180°C the properties are quite stable with a slight decrease in strength.

The high value of compressive strength and the hardness over time of the cement matrix has to be related with the initial homogeneity of the dry blend and the low water content of the slurry.

Cement cores after curing were stored in pressured cell filled with different water qualities included deionised water, sea water, seawater in presence of 10% sulfur gas H<sub>2</sub>S and sea water with 50% gasoil.

Geometrical variations of the cement cores are represented in Table 2.2 in case of the more aggressive solutions that are deionised water, seawater and seawater with sulfur gas. Compressive strengths value variations over time are shown in Table 2.3. After one year of aging period, an increase of the weight with a maximum of 3% with simultaneously, compressive strength increase of 30% was recorded.

*Table 2.2: Weight variation with RPC slurry, durability at 120°C in various aging solutions*

Time	Weight variation %		
	Deionised water	Sea water	Sea water + H <sub>2</sub> S
15 days	0.3	0.75	0.7
1 month	0.5	1.3	1.3
3 months	0.4	1.6	1.6
6 months	1.4	3.4	3
1 year	-	2.7	2.4

*Table 2.3: Compressive strength variation with RPC slurry, durability at 120°C in various aging solutions*

Time	Compressive strength variation with RPC slurry (MPa)			
	Deionised water	Sea water	Sea water + H <sub>2</sub> S	Sea water + gasoil
15 days	117	135	101.5	152
1 month	129	150	150	141
3 months	93	119	111	-
6 months	139	167	163	164
1 year	159	185	183	181

## 2.6 *ThermaLock* cement, an improved CO<sub>2</sub> resistant cementitious material

The U.S. Department of Energy's Brookhaven National Laboratory, in collaboration with Halliburton Company and Unocal Corporation organized and conducted a program to develop and test lightweight, low-cost and CO<sub>2</sub>-resistant under high temperature conditions, non-Portland based cementitious materials, (Weber et. al. 1998, Sugama 1998, 2000, Kuckacka et. al. 1994, 1995a, 1995b, Sugama et. al. 1992, Kuckacka 1991a, 1991b). Known as *ThermaLock* cement, the result product is suited for use in geothermal wells. It can also be applied in oil and gas wells for soil remediation.

### 2.6.1 Design criteria

Design criteria established by industry and ranked in order of importance are as follows (Sugama 1998, 2000, Kuckacka et. al. 1994, 1995a, 1995b, Sugama et. al. 1992, Kuckacka 1991a, 1991b):

- Compatible with conventional field placement technologies
- Carbonation rate < 5 % after 1 year in brine at 300° C containing 500 ppm CO<sub>2</sub>
- Compressive strength > 5 MPa at 24 hours age
- Slurry density < 1.2 g/cc

Other important characteristics needed are:

- Life expectancy 20 years
- Pumpability of ~4 hr at > 100°C
- Bond strength to steel > 70 kPa
- H<sub>2</sub>O permeability < 0.1 m Darcy

*ThermaLock* cement creates zeolite and calcium phosphate minerals that block the carbonation.

### 2.6.2 Materials

*ThermaLock* cement is made mostly of recycled fly ash, the by-product of coal combustion. In addition to fly ash, the formula for the cement includes calcium aluminate, sodium polyphosphate and water in compositions that vary with the depth at which the cement will be used.

The material is formed by acid-base reactions between calcium aluminate compounds and phosphate-containing solutions, mixed with lightweight fillers (Kuckacka et. al. 1995a).

Four commercially available calcium aluminate cements (CAC), Refcon (RE), Luminite (LU), Secar 80 (#80), and Secar 41 (#41), were used as the base solid. Lehigh Portland Cement Company supplied the first two; LaFarge Calcium Aluminates Company supplied the others (Kuckacka et. al. 1994, 1995a, 1995b). The chemical constituents of the RE as determined by x-ray powder diffraction consist of three major phases: monocalcium aluminate [CaO.Al<sub>2</sub>O<sub>3</sub>] (CA), gehlenite [2CaO.Al<sub>2</sub>O<sub>3</sub>.SiO<sub>2</sub>] (C<sub>2</sub>AS), and monocalcium dialuminate [CaO.Al<sub>2</sub>O<sub>3</sub>] (Ca<sub>2</sub>). In contrast, the #80 has CA and CA<sub>2</sub> as its major components and C<sub>2</sub>AS as a minor one

An ammonium polyphosphate fertilizer solution, known as Poly-N (fertilizer grade: 11-37-0, Arcadian Corporation) was employed as the acid liquid reactant (Kukacka et. al. 1994, 1995a). Later in the research (Kukacka et. al. 1995b), a 30 wt% polybasic sodium phosphate solution of pH 6.15 was preferred as the acid reactant for the formulations. The source of the material was Albright and Wilson Americas.

The incorporation of inorganic and organic microsphere fillers into CPC (Calcium Phosphate Cement) produces a lightweight, moderate strength and durable cement. An aluminosilicate ( $3\text{Al}_2\text{O}_3 \cdot \text{SiO}_2$ )-based hollow microsphere (EX), with a density of 0.67 g/cc and a particle size of 75 to 200  $\mu\text{m}$ , was used (Kukacka et. al. 1994, 1995a, 1995b).

The cement formulation (Sugama 1998) consists finally of 23.7 wt% flyash, 15.8 wt% calcium aluminate cement, 12.6 wt% sodium polyphosphate, 29.1 wt%  $\text{Al}_2\text{O}_3$ -shelled microspheres and 18.8 wt% water.

### 2.6.3 Results of the experimentation

It was determined that the reactivity and resistance to carbonation were dependent upon the chemical composition of the base ingredient. The presence of monocalcium aluminate (CA) and gehlenite ( $\text{C}_2\text{AS}$ ) accelerated the setting of the cement and reduced carbonation. The susceptibility of the various CPC matrices to carbonation was in the following order, #80 > RE > LU > #41.

Sugama (Sugama 1998, Kukacka et. al. 1994, 1995a) gives as example that autoclave exposure for 120 days to a 4 wt%  $\text{Na}_2\text{CO}_3$ -saturated brine solution at 300°C produced no evidence of carbonation or strength retrogression (<0.4wt%  $\text{CaCO}_3$  produced). In contrast, class G cement is severely deteriorated, forming ~10 wt%  $\text{CaCO}_3$  after only 7 days exposure.

The addition of hollow aluminosilicate microspheres to the matrix constituent yields slurries with densities of approximately 1.2 g/cc, and after hydrothermal curing forms  $\text{CO}_2$  resistant cement (compressive strength greater than 6.89 MPa) (Kukacka et. al. 1994, 1995a).

Sugama (Sugama 2000) specifies that the service life of *ThermaLock* cement be estimated about 20 years. In contrast, conventional cements deteriorate after only one year in a harsh environment.

### 2.6.4 Large scale field testing

Since the used materials are abundant and inexpensive, and no technical training is required to make the cement, it is economical compared to conventional cements.

In 1997, large-scale field-testing of the cement began at a geothermal well in Sumatra, Indonesia, operated by Unocal Corporation. This location was chosen for the promising geothermal prospects, though characterized by numerous thermal surface features with particularly corrosive fluids and gases. These surface features include fumaroles, steam vents, hot springs, streams and pools exhibiting acidity (pH < 2),  $\text{CO}_2$  content (up to 99% by weight) and high sulfate concentrations. Geological interpretations of the corrosive

formations indicated likely intersection of these formations by the planned wellbore paths. Halliburton Company supplied the cement for these tests. The field application of the new corrosion-resistant cement was accomplished with standard cementing equipment and techniques (Weber et. al. 1998).

In the first commercial use of the product, in April 1999, the Japan Petroleum Exploration Company used the recent cement to complete the geothermal wells in Kyushu, Japan. The company subsequently used more than 140 tons of the product to build several more geothermal wells.

## 2.7 FCRS, a Flexible Corrosion-Resistant Sealant for acid-gas injection

Halliburton has developed a Flexible Corrosion-Resistant Sealant (FCRS) for CO<sub>2</sub> flood injection wells (Getzlaf 1998, Callahan et. al. 1997). Used in separate field studies conducted at Canadian injection well sites in Alberta and British Columbia, the plastic-like sealant withstood the acid attack of the CO<sub>2</sub> and showed a corrosion resistance that conventional slurries - including Portland cement - lack.

### 2.7.1 Description of the sealant

FCRS is a flexible, synthetic elastomer system and contains latex, a cross-linking agent, cross-linking activators, a cross-linking accelerator, and reinforcing agents. The cement is elastic, resilient, and acid resistant while providing good tensile strength. It was designed to provide high shear strength and can withstand severe pipe expansion and contraction without losing compressive strength or compromising zonal isolation.

Halliburton states that the characteristics of the sealant include (Getzlaf 1998):

- The strength to provide adequate support for pipes, and at the same time, the flexibility to allow for pipe expansion in temperatures ranging from 20 to 121°C;
- The resiliency to endure shifts in temperature and stress during injection, production or work over operations;
- Excellent perforating features;
- A makeup that permits drilling with conventional tooth bits; and
- A composition effecting the penetration of areas not accessible to other slurries.

In the laboratory, the acid-resistance of flexible cement was tested against conventional cements. Sample cores were installed in a perforated stainless steel sampling tube for exposure to CO<sub>2</sub> at 43 to 46°C bottom hole temperature and 182 bar. The samples were exposed to CO<sub>2</sub> for 10 days and 119 days. The evaluated cements included Portland cement formulations and flexible cement formulations. After the exposure periods, gravimetric acid solubility tests were conducted on the sample cores. The flexible cement samples showed no visible effects from the exposure to CO<sub>2</sub> and had the lowest acid-solubility measurements. Sample cores of latex CO<sub>2</sub> resistant conventional cement showed significant damage from the CO<sub>2</sub> exposure and showed the highest acid solubility measurements (cf. Table 2.4).

Table 2.5 lists the results of compressive strength and flexibility tests performed on neat cement and flexible cement.

Table 2.4: Results of Acid Solubility Testing

Cement Composite	15% HCL ambient temp. 10-day exposure	15% HCL ambient temp. 119-day exposure
Premium cement, neat	36%	50%
Premium cement + latex	32%	49%
FCRS + 25% corrosion-resistant cement + 125% silica flour	0.8%	6%

Table 2.5: Compressive and Flexible Strength Tests

Composite	Compressive Strength (bar)	Flexural Strength (bar)
Premium cement, neat	402	37
FCRS	34	72

## 2.7.2 Field application

FCRS compositions have been used effectively to seal old perforations and in conformance of injection profiles in CO<sub>2</sub>-enhanced recovery wells. The sealant is resistant to corrosive fluids, elastic and helps to support pipe securely, while remaining ductile to help permit changes in pipe

### 2.7.2.1 Case #1: Alberta Acid-Gas Injection Well

The Alberta procedure, conducted in 1995, involved using a lightweight, hollow-microsphere cement as the lead slurry, followed by a conventional Class G premium Portland cement, and finally by the FCRS. A stabilizing surfactant was added to the latter section of the Portland phase to avert incompatibility between this stage and the FCRS.

FCRS materials were batch mixed into tanks. The latex, defoamer, surfactant, and liquid accelerator were mixed in the batch mixer. The dry-blended activators, cross-linking agent, and reinforcing materials were added and mixed until the mixture was uniform. To help prevent contamination of the FCRS, the pumping equipment was cleaned with acetic acid, neutralized with soda ash, and rinsed with chlorine-free water. The bulk equipment was then vacuumed and flushed with silica flour.

Figure 2.1 is a schematic illustration of the well condition and Table 2.6 gives some of the well characteristics. Table 2.7 lists the cementing compositions employed along with the actual volumes of fluids and densities pumped during each stage.

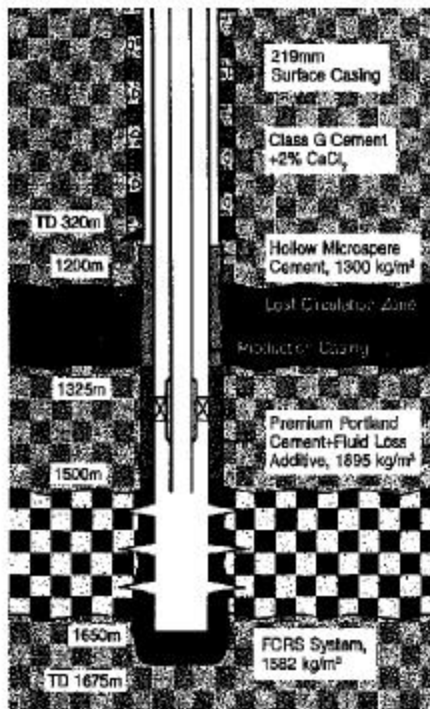


Figure 2.1: This schematic of the completed Alberta injection well displays the various cement zones (Getzlaf 1998)

Table 2.6: Alberta injection well characteristics

Total depth	1677 m
Bottomhole static temperature, BHST	55°C
Bottomhole circulating temperature, BHCT	45°C

Table 2.7: Cementing compositions, actual volumes of fluids and densities pumped for each stage (case # 1, Alberta injection well)

Stage	Slurry volume (m <sup>3</sup> )	Density (kg/m <sup>3</sup> )
Pump water wash	2.914	-
Pump lightweight hollow microsphere cement (lead)	64.415	1300
Pump Class G primary cement (first tail-in cement)	11.422	1895
Pump FCRS (final tail-in cement)	4.778	1582
Pump displacement	19.677	1000
<b>Total/average</b>	<b>103.203</b>	-

### 2.7.2.2 Case #2: British Columbia Acid-Gas Injection well

This well required FCRS to protect the primary cement sheath from the effects of corrosive acids produced by the injection of CO<sub>2</sub> and H<sub>2</sub>S. In the British Columbia operation, which was performed in August 1996, various volumes of thixotropic cement were pumped in as scavenger, lead and tail-in slurries (with the latter portion of the first tail containing a

stabilizing additive) before the FCRS and a top wiper plug were added. Log readings indicated minimal or no loss of integrity in the British Columbia job.

Table 2.8 gives some of the well characteristics.

Table 2.8: *British Columbia injection well characteristics*

Total depth	1480 m
Bottomhole static temperature, BHST	49°C
Bottomhole circulating temperature, BHCT	40°C
Cement interval requiring FCRS	from 1375 to 1482 m

Pre-job testing in the laboratory was performed to determine thickening times, compressive strength, and compatibility. Formulation given in Table 2.9 produces a thickening time of 4.5 hours at 45°C.

Table 2.9: *FCRS blend for #2 (British Columbia acid-gas injection well)*

Component	Percentage %
Polymer	100
Defoamer	3.25
Crosslinking agent	2
Activator	1.95
Corrosion-resistant cement	25
Dispersant	9
Accelerator	0.125
Stabilizer	-
Silica flour	125

The mixing and cleaning procedures were similar to case #1. Table 2.10 lists the cementing compositions employed along with the actual volumes of fluids pumped during each stage.

Table 2.10: *Cementing compositions and actual volumes of fluids pumped for each stage (case # 2, British Columbia injection well)*

Stage	Slurry volume (m <sup>3</sup> )
Pump wash	3 water + 3 diesel
Pump thixotropic cement (scavenger slurry)	3
Pump thixotropic slurry (lead)	17.93
Pump thixotropic slurry + stabilizer (first tail-in slurry)	6.8
Pump FCRS (final tail-in cement)	2.5

Log data collected from the well in September 1996 indicated good displacement and bond integrity (Callahan et. al. 1997).

### 2.7.2.3 Case #3: Second well in British Columbia

Another well, completed in British Columbia in 1997, was successfully treated with FCRS preceded by lead slurry of pozzolanic cement and a surfactant, followed by a wiper plug and the FCRS. Figure 2.2 shows the use of pozzolan lead cement in the well.

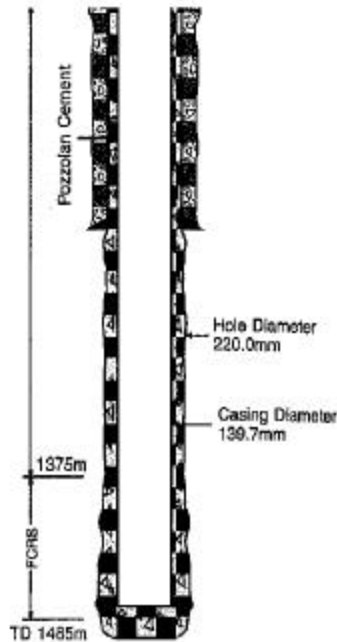


Figure 2.2: The use of pozzolan lead cement is shown here in a second British Columbia well that was completed in 1997 (Getzlaf 1997)

## 2.8 An Epoxy solution

Maepoxy UV-L, product from Rescon Mapei, is a dissolvent free epoxy solution suited for use under water. Maepoxy UV-L is based on a low viscosity resin of epoxy and polyamide hardening agent.

### 2.8.1 Technical data and operating instructions

A few data is listed below (Rescon Mapei):

Dry solids content:	approx. 98%
Density of mixture:	1.4 kg/l
Colour:	light blue (white resin, dark blue hardening agent)
Lowest application temp.:	+ 5 °C (in water)
Workability of mix:	at +20°C: 30-40 mn at +10°C: 50-60 mn
Curing time:	at +15°C: 5-7 days at +5°C: 1-2 weeks
Compressive strength:	at +20°C 7 days: 70 MPa
Flexural strength:	at +20°C 7 days: 7 MPa
Modulus of elasticity:	approx. 17 500 MPa
Electric conductivity:	non-conducting

Mixing ratio: 12 : 3  
Packaging: 5.0 and 15.0 kg  
Storage: use by date of 1 year, stored frost free in original packaging

The components should be at the temperature between +15°C and +25°C for the mixing procedure. Stir component B, the hardening agent and add component A, the epoxy resin, in the mixer. Mix for 3-4 minutes with a drill at low speed. The final mixture is a light blue, homogeneous mass.

According to Rescon Mapei, Mapepoxy UV-L is a long-term durability product and has very good resistance against corrosion. As a low viscosity material, it will adapt easily down in the borehole. It has a very good resistance against different chemicals, including oil and gas, for an environment temperature less than 100°C.

Mapepoxy UV-L was used to seal the annulus through the wellhead in the case of gas leakage for Gullfaks. The borehole was filled with cement slurries and the Mapepoxy UV-L was used in the annulus through the wellhead. Pressurization was used to hold the product.

## 2.9 Conclusion

Special CO<sub>2</sub> resistant cements are provided that has better resistance against CO<sub>2</sub> compared to standard cements. Adding silica flour and others additives in various proportions increase the durability of the cement and its resistance in a corrosion environment. Nevertheless, at best, such cementitious materials only postpone the inevitable.

The reactive powders cement, RPC, developed by the Institut Français du Pétrole has shown better durability properties compared to traditional materials. Nevertheless the weight lost by the cement cores in aggressive solutions remains important.

Brookhaven National Laboratory, in collaboration with Halliburton Company and Unocal Corporation has developed a lightweight, low-cost and CO<sub>2</sub>-resistant *ThermaLock* cement. The result product is suited for use in geothermal wells. The service life of *ThermaLock* cement is to be estimated about 20 years.

The flexible corrosion-resistant sealant, FCRS, a non-Portland annular sealant for acid-gas injection developed by Halliburton and being used in CO<sub>2</sub> flood operations, was applied to two acid-gas wells in western Canada to help provide zonal isolation and protect the integrity of the cement sheath. Halliburton states that this sealant can withstand the corrosive environment encountered in both primary and remedial cementing operations in acid-gas injection and CO<sub>2</sub>-enhanced recovery projects. Nevertheless long term experiments on the resistance of the sealant to a hard CO<sub>2</sub>/brine environment are missing.

The Mapepoxy UV-L, developed by Rescon-Mapei, seems to be a quite promising alternative to traditional cement and even to advanced cementitious materials. Unfortunately and so far there is no information about the long term durability and CO<sub>2</sub>/brine resistance for this product. Test analyses of some Mapepoxy UV-L samples removed from the Gullfaks field should be conducted in order to measure the acid-resistance of the product and its long-term durability in harsh environment. The new

materials discussed here have not been exposed for long duration tests in CO<sub>2</sub>/brine environment.

### 2.9.1 Recommendations for further work

During the next year, Sintef Petroleum Research proposes to conduct some long-term tests analysis on different material in order to estimate their durability in a CO<sub>2</sub>/brine environment at high pressure and high temperature. Several materials should be tested, included:

- RPC (the reactive powders cement developed by the Institut Français du Pétrole),
- *ThermaLock* cement (developed by the Brookhaven National Laboratory),
- FCRS (a Flexible Corrosion-Resistant Sealant developed by Halliburton),
- Mapepoxy UV-L (developed by Rescon-Mapei),
- A magnesia phosphate based cement namely ASR-1 supplied by FEB International plc, Manchester, UK (Frantzis 2003).

### 3 Simulations

#### 3.1 Objective

To estimate the risk of CO<sub>2</sub> escape from a leaky abandoned well and quantify the escape as an emission profile.

#### 3.2 Model

A large underground sandstone reservoir was selected as a case for studying possible escape. The sealing layer has a relatively flat topography with height variation less than 50 meters. The model has a single injection well and a single abandoned well which sealing integrity is manipulated in numerical simulations to see what effect it make on the retention of injected CO<sub>2</sub>. In the formation an abandoned well is located a few hundred meters from the well used for CO<sub>2</sub> injection. This well is plugged but may still be a potential escape route for CO<sub>2</sub> trough the sealing layer since CO<sub>2</sub>/brine may erode the cement plugs and steel casings; see e.g. (Lindeberg 2001, Lindeberg et. al. 2002). At present details on this deterioration (e.g. erosion rate, permeability of remaining material) is not known to such a degree that it can be modelled. Therefore a sensitivity study for different reservoir/well parameters was performed. The main purpose was to get an estimate of the potential importance of leakage trough such a well and some information regarding what is most important to study in this respect: details of the CO<sub>2</sub> erosion of the well or simulations of the whole reservoir. In all cases initially 24 million tonnes CO<sub>2</sub> was injected near the bottom of the reservoir.

The base case model had a horizontal permeability  $k_x = k_y = 2000$  mD and vertical permeability  $k_z = 200$  mD. The corner point simulation grid has  $N_x = 73$ ,  $N_y = 96$ , and  $N_z = 52$  grid cells with dimensions  $L_x = L_y = 100$  m, and  $L_z \sim 5$  m respectively (Figure 3.1).

#### 3.3 Base case

It was assumed that the well under consideration was completely closed such that no CO<sub>2</sub> could escape from the reservoir. The CO<sub>2</sub> injected will then first migrate upwards and settle at the top of the reservoir as a bubble. Here the topography of the sealing layer will be important for the horizontal CO<sub>2</sub> flow. The CO<sub>2</sub> will slowly dissolve in the water as shown in Figure 3.2. Since water with dissolved CO<sub>2</sub> has higher density than the original water it will eventually fall to the bottom again. This process takes several hundred years, but is essential for the long time scales we study. This physics is therefore included in our simulations. The thickness of the CO<sub>2</sub> bubble is at the maximum 20-30 m but shrinks gradually to zero after  $\sim 2000$  years.

The most important question is therefore related to whether the plugs will be penetrated due to erosion during the time the CO<sub>2</sub> is at the top of the reservoir. If they are penetrated one may also ask how much of the CO<sub>2</sub> will escape through the well before it is dissolved in water and sinks to the bottom.

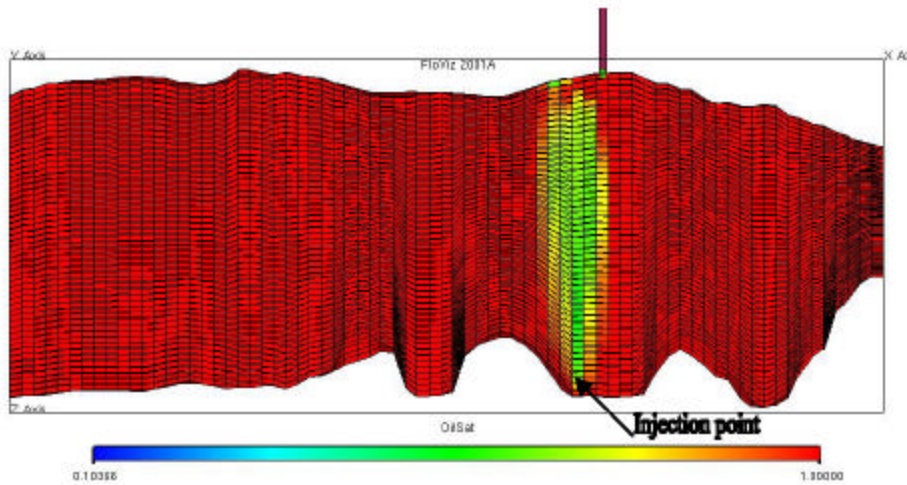


Figure 3.1 This is a cross section of the grid showing the oil saturation 5 years after the start of CO<sub>2</sub> injection. Note also the production well, here perforated in the uppermost grid cell (K=1) only. This well is placed very near a high point of the sealing layer, i.e. a place of high CO<sub>2</sub> concentration.

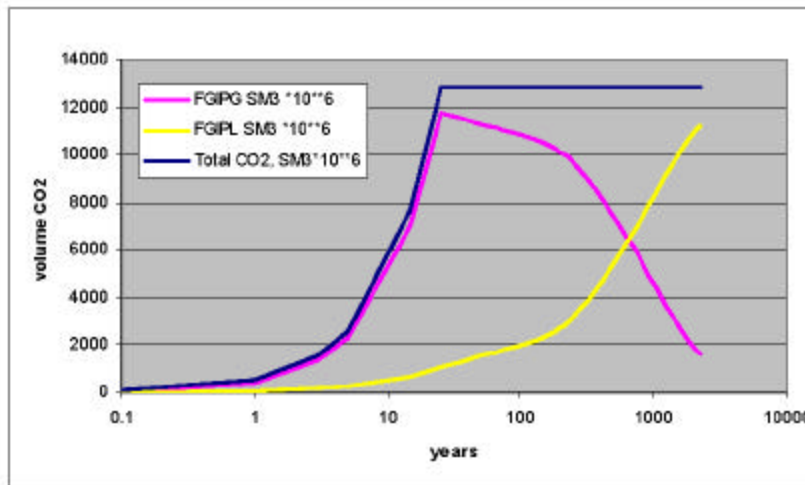


Figure 3.2 Free CO<sub>2</sub> (FGIPG) and CO<sub>2</sub> dissolved in water (FGIPL) as function of time after start of CO<sub>2</sub>-injection.

### 3.4 "Worst case scenario"

Here the well tubing is assumed to be open the whole way up to the surface and it is perforated in the upper grid cell, i.e. about the upper 5 m of the reservoir. The well is controlled on bottom hole pressure (BHP) assuming hydrostatic pressure at the reservoir surface. The ratio of escaped CO<sub>2</sub> to the injected CO<sub>2</sub> as function of time is shown in

\\Boss\IK54523200R\rapport\SMORapp\_Jan2003\_v3.doc\120.18.02.03

Figure 3.3. We note that about 60% of the injected CO<sub>2</sub> has escaped after ~ 200 years and very little after this. The remaining CO<sub>2</sub> will dissolve in the water and sink to the bottom of the reservoir. Here it will remain “forever”.

It is also interesting to see how the results change if we let the well be perforated in both cell K=1 and K=2, i.e. about 10 m from the top of the reservoir. The results are shown in Figure 3.4. As expected more of the CO<sub>2</sub> escapes when the well has a longer perforated interval. However, the difference is not large.

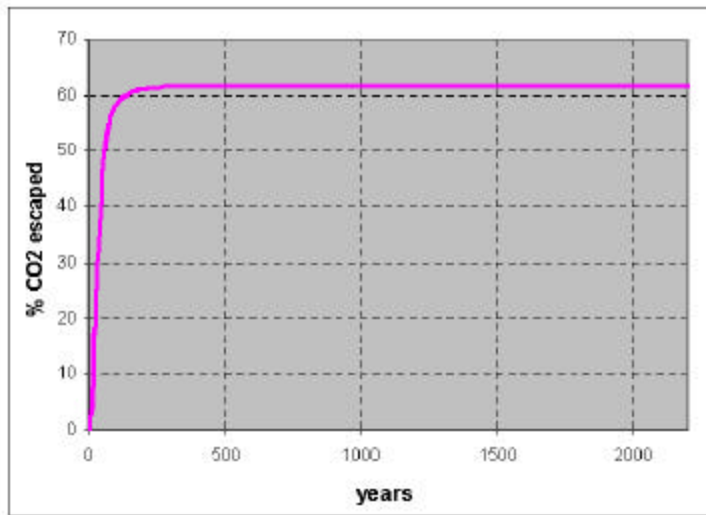


Figure 3.3 The figure shows the ratio of escaped CO<sub>2</sub> to the injected CO<sub>2</sub> as function of time. The well is perforated in the uppermost grid cell, i.e. about the upper 5 m.

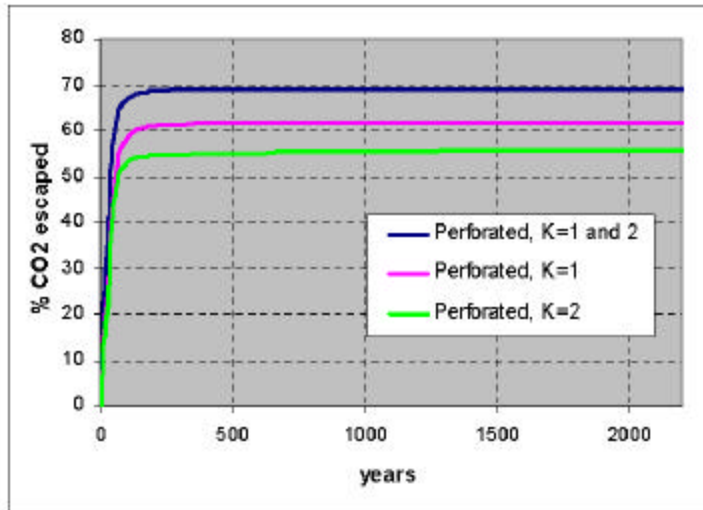


Figure 3.4 Ratio of escaped CO<sub>2</sub> to injected CO<sub>2</sub> as function of time for different well perforations.

### 3.5 Reduced productivity

The above “worst case scenario” may not be realistic since we assume that the whole height of the grid cell just below the sealing layer is open for production. We have therefore done some simulations with reduced productivity, i.e. we have multiplied the well transmissibilities with 0.01 and 0.0001 respectively. This corresponds to wells which are not completely open, but where some of abandonment seal is only partially deteriorated and still provide some restraint towards fluid escape. The CO<sub>2</sub> escaped from the reservoir as a function of time is shown in Figure 3.5. We see that about 18% escapes for productivity reduction of 0.01 while less than one percent escapes for productivity reduction of 0.0001.

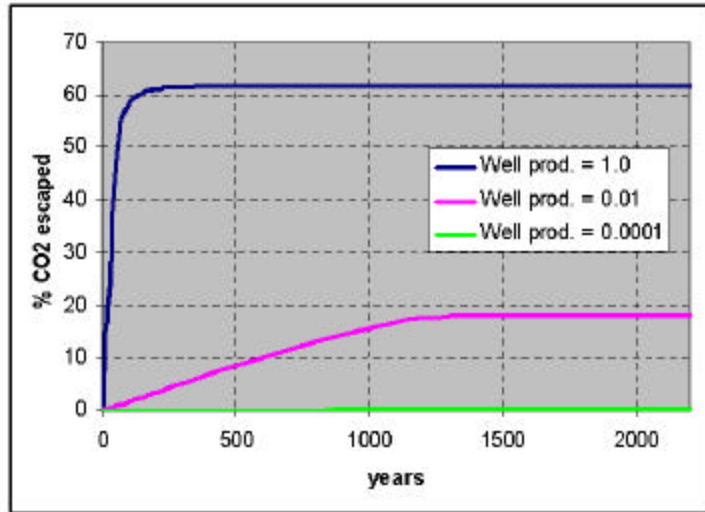


Figure 3.5 The effect of reduced well productivity on escaped CO<sub>2</sub> versus time.

### 3.6 Constant water rate

An alternative to controlling the well by bottom hole pressure (BHP) is to use a constant water rate. We tried  $Q_{water} = 1.0 \text{ sm}^3/\text{day}$  as shown in Figure 3.6. This is however a rather unrealistic well control scenario.

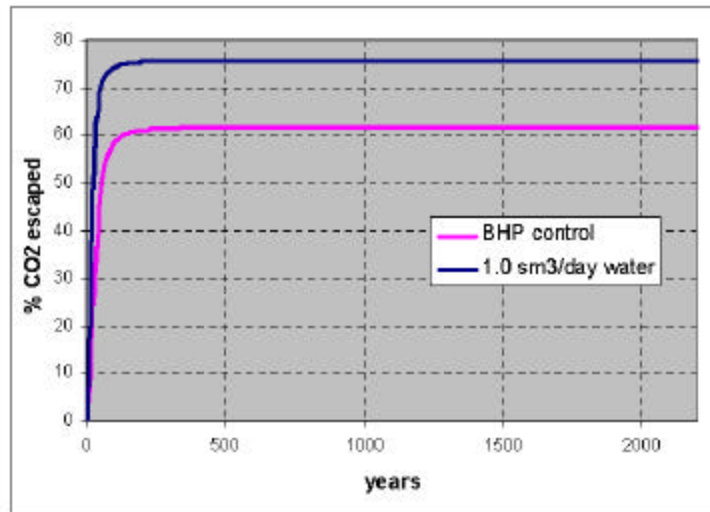


Figure 3.6 Comparison of BHP and constant rate well control.

### 3.7 Coarsened grid

To reduce simulation time it is possible to use a coarsened grid in unimportant regions. However, there were problems running such jobs in parallel. We also studied the effect of global grid coarsening. The results are shown in Figure 3.7. The influence on the remaining volumes of CO<sub>2</sub> is rather small but the simulation times are (as expected) drastically reduced.

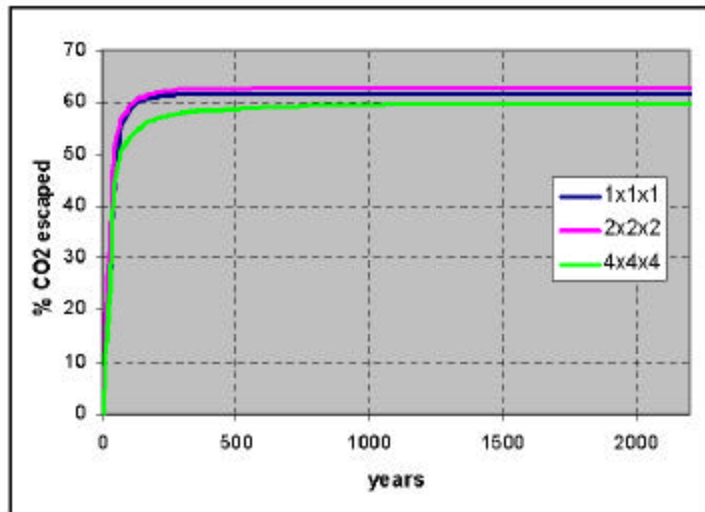


Figure 3.7 Comparison of coarsened grids with cells of approximately  $2 \times 2 \times 2 = 8$  cells and  $4 \times 4 \times 4 = 64$  cells. We observe that the influence on the remaining volumes of CO<sub>2</sub> is rather small. The simulation times are drastically reduced from  $83745 \times 10$  s (10 CPUs)  $\rightarrow$  15716 s  $\rightarrow$  1911 s.

### 3.8 Reduced vertical permeability

The vertical permeability will clearly influence on how fast the CO<sub>2</sub> will move up and down in the reservoir. This will influence on the CO<sub>2</sub> escaping through the well, as shown in Figure 3.8. However, a reduction in vertical permeability by a factor of 10 will only change the remaining CO<sub>2</sub> by ~25%.

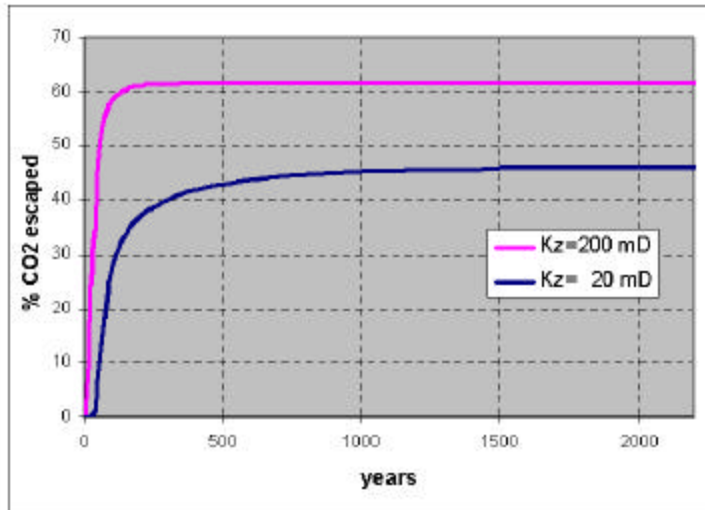


Figure 3.8 Reducing the permeability from 200 mD to 20 mD reduces the escape of CO<sub>2</sub>. Even if this reduction is by a factor of 10 the change in remaining CO<sub>2</sub> is only ~25%.

### 3.9 Recommendations for future work

The simulations have shown that the most important factor regarding CO<sub>2</sub> escape from the reservoir is the details of the erosion process of the cement/steel used in the well, not the details of the reservoir. The future work should therefore concentrate on getting a better understanding of this erosion process and obtain better estimates for e.g. erosion rates as function of aquifer drift speed and concentration of dissolved CO<sub>2</sub> in water. Only after such estimates are available, simulations of the full reservoir performance should be continued. Then the simulation should be run with a time varying well productivity. It is also probably necessary to get a better understanding of the well flow performance from the reservoir to the surface since some eroded cement will probably be left in the well bore.

## References

- Callahan, T., Getzlaf, D., Onan, D.: "Non-Portland Annular Sealant for Acid-Gas Injection", 7th Bien CADE/CAODC Spring Drilling Conf (Calgary, CAN, 4/8-10/97) Proc Pap No 97-136, 1997.
- Frantz, P., Baggot, R.: "Transition Points in Steel Fibre Pull-out Tests from Magnesium Phosphate and Accelerated Calcium Aluminate Binders", *Cement and Concrete Composites*, V. 25, issue 1, PP 11-17, January 2003.
- Getzlaf, D.: "Field Studies Illustrate Merits of FCRS (Flexible Corrosion-Resistant Sealant)", *Amer Oil Gas Reporter* V. 41, No 13, PP 95-96,105, December 1998.
- Ivashov, V.I.: "Cement Dust Used As Steel Corrosion Inhibitor - Is Obtained from Electrostatic Filters and Prevents Corrosion from Petroleum and Mineralised Water", USSR 1826996-A3, P 7/7/93, F 7/27/90 (APPL 4885992) (C23F-011/00) SOVIET PAT ABSTR NO 9501, PP 3-H - 4-H, 2/3/95, 1993.
- Kukacka, L.E., Sugama, T.: "Lightweight CO<sub>2</sub>-Resistant Cements for Geothermal Wells Completions", Brookhaven Nat. Lab. Rep No BNL-61259 (DE95005965), 1995.
- Kukacka, L.E., Sugama, T.: "Lightweight CO<sub>2</sub>-Resistant Cements for Geothermal Wells Completions", Brookhaven Nat. Lab. Rep No BNL-60326 (DE94011731), 1994.
- Kukacka, L.E., Sugama, T.: "Recent Advances in the Development of Lightweight CO<sub>2</sub>-Resistant Well Cements", Brookhaven Nat. Lab. Rep No BNL-62607 (DE96007741), 1995.
- Kukacka, L.E.: "Geothermal Materials Development: FY 1990 Accomplishments and Current Activities", Brookhaven Nat. Lab. Rep No BNL-45995 (DE91015146), January 1991.
- Kukacka, L.E.: "Geothermal Materials Development", Brookhaven Nat. Lab. Rep No BNL-47529 (DE92016940), December 1991.
- Liao, G., Yang, Y., Wang, H.: "Effect on Anti Corrosion Ability of Oil Well Slurry Using Silica Flour", *Oil Drilling Prod Technol* V 18, No 4, PP 31-34, 43, 106, 8/20/1996.
- Lindeberg, E., Moen A., Justnes, H., Drugli, J.M., Rogne, T.: "Mid-term report June 2002: The Long Term Sealing Capacity of Cemented Petroleum Wells in a CO<sub>2</sub> Storage Project", September 2002.
- Lindeberg, E.: "The Risk of Leakage from Abandoned Petroleum Wells in CO<sub>2</sub> Storage Project", December 2001.
- Noik, Ch., Rivereau, A.: "Oil well cement durability", Institut Français du Pétrole, SPE 56538.
- Novokhatskii, D.F., Tikhonov, V.G.: "Hydrogen Sulfide-Resistant Plugging Materials", *Stroit Neft Gaz Skvazhin Sushe More* No 3, PP 28-31, March 1999.
- Rescon Mapei: Mapepoxy UV-L, Undervannslim, Internet page: <http://www.rescon.no/>
- Sugama, T., Carciello, N.R.: "Carbonation of Hydrothermally Treated Phosphate-Bonded Calcium Aluminate Cements", *Cement Concrete Res* V 22, No 5, PP 783-792, September 1992.
- Sugama, T.: "Brookhaven Lab, Halliburton Company and Unocal Corporation Win R&D 100 Award for High-performance Cement", News release from the Brookhaven National Laboratory, Internet page, August 2, 2000.
- Sugama, T.: "CO<sub>2</sub>-Resistant Cements in Geothermal Wells", Internet page from the U.S. Department of Energy, Geothermal Energy Technical Site, 1998.

Weber, L., Emerson, E., Harris, K., Brothers, L.: "*The Application of a New Corrosion Resistant Cement in Geothermal Wells*", Annu. Geotherm Resources Council MTG (San Diego, 9/20-23/1998) Trans V 22, PP 25-30, 1998.

Yao, X.: "*CO<sub>2</sub> Corrosion on Oilwell Cement Sheath: Thermodynamic Criteria, Corrosive Mechanism and Prevention*", Journal Southwest Petroleum Inst. V 20, No 3, PP V 68-71, August 1998.

### **2.3.3 Geomechanical Effects of CO<sub>2</sub> Storage**

Report Title

**CO<sub>2</sub> Capture Project - An Integrated, Collaborative Technology Development Project for Next Generation CO<sub>2</sub> Separation, Capture and Geologic Sequestration**

**Geomechanical Effects of CO<sub>2</sub> Storage**

Report Reference

**2.3.3**

Type of Report:	Semi-Annual Report
Reporting Period Start Date:	February 2003
Reporting Period End Date:	July 2003
Principal Author(s):	Dan Ebrom
Date Report was issued:	August 2003
DOE Award Number:	DE-FC26-01NT41145
Submitting Organization:	BP North America Inc.

Disclaimer

This report was prepared as an account of work sponsored by an agency of the United States Government. Neither the United States Government nor any agency thereof, nor any of their employees, makes any warranty, express or implied, or assumes any legal liability or responsibility for the accuracy, completeness or usefulness of any information, apparatus, product, or process disclosed, or represents that its use would not infringe privately owned rights. Reference herein to any specific commercial product, process, or service by trade name, trademark, manufacturer, or otherwise does not necessarily constitute or imply its endorsement, recommendation, or favoring by the United States Government or any agency thereof. The views and opinions of authors expressed herein do not necessarily state or reflect those of the United States Government or any agency thereof.

### **2.3.3.1 Abstract**

The aim of the study is to evaluate techniques for measuring the flux of CO<sub>2</sub> from the earth's surface, focusing on the eddy-covariance technique and its potential application to monitoring underground CO<sub>2</sub> reservoirs.

A report will be written based on a review of existing experimental and theoretical studies. The report shall include: the basic principles of the eddy-covariance technique for measuring turbulent fluxes in a micrometeorological environment; sensor-design criteria for application to CO<sub>2</sub> fluxes and mixing ratios measured in the atmosphere near the earth's surface; discussion of the merits of commercially available sensors and eddy-covariance system components; the use of the technique in horizontally homogeneous applications, such as over crop fields and forest canopies; the application of the eddy-covariance technique to isolated sources via the source "footprint" concept; discussion of our recent experience with the footprint technique in geothermal regions; possible complications of extending this technique to complex terrain; expected measurement precision and detection limits.

## 2.3.3.2 Table of Contents

2.3.3.1 Abstract.....	968
2.3.3.2 Table of Contents .....	969
2.3.3.4 Introduction.....	970
2.3.3.5 Experimental.....	970
2.3.3.6 Results and Discussion.....	970
2.3.3.7 Conclusion.....	970
2.3.3.8 References .....	970

### **2.3.3.4 Introduction**

The goal of the project is to produce a report that documents the predicted stress effects on, and responses by, both reservoirs and seals resulting from storage of CO<sub>2</sub> in geological formations.

In particular, to study the expected geomechanical responses of both reservoirs and seals, and the optimum technologies for verification of geomechanical responses, and in particular technologies for early leak detection.

### **2.3.3.5 Experimental**

No experimental methods are being used for the research.

### **2.3.3.6 Results and Discussion**

Deliverables will be:

1. Brief discussion of CO<sub>2</sub> storage processes, concentrating on the likely changes in stress fields in the reservoir and the seal.
2. Discussion of seal characterisation especially relating to seal capacity measurement
3. Discussion of the factors controlling geomechanical changes which are predicted to occur, with a focus on likelihood of induced seismicity, fault reactivation and fault or fracture initiation, and measures to be taken to reduce likelihood.
4. Discussion of Monitoring technologies available and the underlying changes in physical/chemical properties being measured, concentrating on those that appear most suitable to detect changes in stress in both the reservoir and seal, again with a focus on induced seismicity.
5. Review of technologies that appear suitable for early leak detection.

### **2.3.3.7 Conclusion**

This report was contracted in July 2003 and work is underway, but no conclusions have been drawn at this time.

### **2.3.3.8 References**

Not applicable.

## **2.4 Monitoring**

### **2.4.1 Monitoring Systems for Small Leakage Rates**

Report Title

**CO<sub>2</sub> Capture Project - An Integrated, Collaborative Technology Development Project for Next Generation CO<sub>2</sub> Separation, Capture and Geologic Sequestration**

**Monitoring Systems for Small Leakage Rates**

Report Reference

**2.4.1**

Type of Report: Semi-Annual Report

Reporting Period Start Date: February 2003

Reporting Period End Date: July 2003

Principal Author(s): Yongchun Tang and Patrick J. Shuler

Date Report was issued: August 2003

DOE Award Number: DE-FC26-01NT41145

Submitting Organization: Tang Associates

Address: Attention: Yongchun Tang  
1904 Tambor Court  
Rowland Heights, CA 91748

Disclaimer

This report was prepared as an account of work sponsored by an agency of the United States Government. Neither the United States Government nor any agency thereof, nor any of their employees, makes any warranty, express or implied, or assumes any legal liability or responsibility for the accuracy, completeness or usefulness of any information, apparatus, product, or process disclosed, or represents that its use would not infringe privately owned rights. Reference herein to any specific commercial product, process, or service by trade name, trademark, manufacturer, or otherwise does not necessarily constitute or imply its endorsement, recommendation, or favoring by the United States Government or any agency thereof. The views and opinions of authors expressed herein do not necessarily state or reflect those of the United States Government or any agency thereof.

### **2.4.1.1 Abstract**

This project just has begun in mid-July 2003, following the recent execution of a contract agreement with BP. The project plans calls for completion by October 31, 2003.

The objective of this project is to perform calculations that will estimate the capability of various ground-level analytical instruments to monitor for leakages of carbon dioxide associated with a subsurface injection sequestration project. In particular, our focus will be to assess the ability of ground-level instruments to detect successfully the leakage of as little as 1% of the total carbon dioxide injected into the subsurface. This new project is a follow-up to a previous desk study for the CCP Consortium in which Tang Associates provided a survey of current and potential carbon dioxide monitoring technologies.

## 2.4.1.2 Table of Contents

2.4.1.1 Abstract.....	973
2.4.1.2 Table of Contents .....	974
2.4.1.3 Introduction.....	975
2.4.1.4 Executive Summary.....	976
2.4.1.5 Experimental / Planned Methodology.....	977
2.4.1.5.1 Work Plan.....	977
2.4.1.5.2 Deliverables .....	977
2.4.1.6 Results and Discussion.....	977
2.4.1.7 Conclusion.....	977
2.4.1.8 References .....	978

### **2.4.1.3 Introduction**

One of the greatest challenges in a subsurface carbon dioxide sequestration project is to verify that this greenhouse gas is injected successfully and remains in fact below ground and does not leak back into the atmosphere. Such subsurface injection projects typically occupy several or more square miles and have many potential sources of leaks, such as in the surface facilities, from the wellbores, and via migration through the strata back to the surface. Another important consideration is that the monitoring program must be planned to be reliable over a time frame of many years.

Tang Associates provided a paper study to the CCP Consortium in 2002 concerning various instruments capable of measuring atmospheric carbon dioxide concentrations. A number of commercially available instruments were identified, as well as some potential new technologies for monitoring for leakages of carbon dioxide associated with a sequestration project (Reference 1).

The CCP Consortium has agreed to sponsor Tang Associates to conduct a follow-up desk study to assess the capability of existing ground-level instruments (and also analytical instruments that could become available based on new technology) to monitor successfully leakages of carbon dioxide associated with a subsurface disposal project. In particular, CCP has the objective of being able to detect a leakage of 1% or less of the total carbon dioxide sequestered back into the atmosphere. We will perform a series of calculations to answer the question that with the sensitivities of the instruments identified in our previous report to CCP, what level of carbon dioxide leakage could be detected. Several anticipated scenarios for carbon dioxide leaks and design of monitoring programs will be considered and evaluated in this study. The calculations will be organized into an Excel spreadsheet file. This computer software will be a user-friendly tool that others may use to study the anticipated sensitivity of their particular carbon dioxide monitoring program subsequent to the completion of this project

#### **2.4.1.4 Executive Summary**

This project just has begun in mid-July 2003, following the recent execution of a contract agreement with BP. The work plan has project completion slated by October 31, 2003.

The objective of this project is to perform calculations that will estimate the capability of various ground-level analytical instruments to monitor for leakages of carbon dioxide back into the atmosphere. Loss of injected carbon dioxide is a long-term risk associated with any subsurface injection sequestration project. In particular, our focus will be to assess the ability of a package of ground-level instruments to detect successfully the leakage of as little as 1% of the total amount of carbon dioxide injected into the subsurface back into the atmosphere.

This new project is a follow-up to a previous desk study for the CCP Consortium completed in February, 2002, in which Tang Associates provided a survey of current and potential atmospheric carbon dioxide measurement technologies (Reference 1). This survey included a description of various instruments, and their detection limits and sensitivities. This information is some of the input data required for this new study which is now just started.

The project plan includes writing software code (Excel, spreadsheet program) that will calculate the detection limit for carbon dioxide leakage into the atmosphere at ground level for a given instrument monitoring program and gas leakage scenario. The final report will include several worked examples.

## **2.4.1.5 Experimental / Planned Methodology**

### **2.4.1.5.1 Work Plan**

Our previous report to the CCP Consortium (Reference 1) includes a description of a number of ground-level commercial instruments for the detection of carbon dioxide concentrations in air. Vendors of these instruments that are designed for point detection of carbon dioxide concentration provide specifications for instrument accuracy, lower limit of detection, and precision. Based on these instrument specifications and making a series of assumptions concerning the sequestration project operation (such as the source of leak, detector location, weather conditions, etc.), one can estimate at what level of carbon dioxide leakage these instruments could successfully identify a problem. We will consider only an analysis of subsurface injection sequestration projects under several different operating/leakage scenarios. The target the CCP Consortium has set for a ground-level monitoring system is that it be able to identify reliably as little as leakage of 1% of the entire volume of injected carbon dioxide.

This same mathematical analysis will be performed for experimental/developmental instruments such as the laser-based detection system proposed in our previous report (Reference 1). For these instruments where the detection characteristics are not yet established; we will use estimated lower and upper ranges of instrument performance in the analysis of its capability for detection of carbon dioxide leakages in a field project.

The required calculations should lend themselves to being organized into an Excel spreadsheet program. The software will be made fairly simple with sufficient documentation so that other users may be able to calculate conveniently the capability of a carbon dioxide detection program with their own input parameters for instrument specifications and sequestration project leakage scenarios.

### **2.4.1.5.2 Deliverables**

1. A spreadsheet program that performs calculations for the capability of leakage detection of carbon dioxide, given an instruments performance specifications and the assumed operating conditions of a subsurface sequestration project.
2. Several worked examples that illustrate the use of the spreadsheet program. Calculate in these examples the capability of different instruments to detect a 1% leakage of carbon dioxide for several different sequestration project scenarios.
3. A written report documenting this work.

## **2.4.1.6 Results and Discussion**

None at this time.

## **2.4.1.7 Conclusion**

None at this time.

### **2.4.1.8 References**

1. Tang Associates, report to CCP: “Atmospheric CO<sub>2</sub> Monitoring Systems --- A Critical Review of Available Techniques and Technology Gaps”, February, 2002.

## **2.4.2 Investigation of Novel Geophysical Techniques for Monitoring of CO<sub>2</sub> Migration**

Report Title

**CO<sub>2</sub> Capture Project - An Integrated, Collaborative Technology Development Project for Next Generation CO<sub>2</sub> Separation, Capture and Geologic Sequestration**

Project Title:

**Investigation of Novel Geophysical Techniques for Monitoring of CO<sub>2</sub> Migration**

Report Reference

**2.4.2**

Type of Report:	Semi-Annual Report
Reporting Period Start Date:	February 2003
Reporting Period End Date:	July 2003
Principal Author(s):	Erika Gasperikova G. Mike Hoversten
Date Report was issued:	August 2003
DOE Award Number:	DE-FC26-01NT41145
Submitting Organization:	Lawrence Berkeley National Laboratory
Address:	One Cyclotron Road MS: 90R1116 Berkeley, CA 94720

This report was prepared as an account of work sponsored by an agency of the United States Government. Neither the United States Government nor any agency thereof, nor any of their employees, makes any warranty, express or implied, or assumes any legal liability or responsibility for the accuracy, completeness or usefulness of any information, apparatus, product, or process disclosed, or represents that its use would not infringe privately owned rights. Reference herein to any specific commercial product, process, or service by trade name, trademark, manufacturer, or otherwise does not necessarily constitute or imply its endorsement, recommendation, or favoring by the United States Government or any agency thereof. The views and opinions of authors expressed herein do not necessarily state or reflect those of the United States Government or any agency thereof.

**Disclaimer**

### 2.4.2.1 Abstract

A number of different geophysical techniques are considered in this project. Seismic, gravity, electromagnetic and streaming potential (SP) geophysical techniques are being considered as CO<sub>2</sub> monitoring tools in this study. To date, seismic, gravity and SP have been modeled and will be considered in this report. Numerical modeling has been done on flow simulations based on a proposed CO<sub>2</sub> sequestration project on the North Slope of Alaska as well as a project in South Texas (to be begun in fall 2003). The SP modeling done for the project is more limited than the other geophysical techniques because the SP modeling codes are restricted to steady state injection in 2D whereas all other geophysical modeling is three-dimensional. The SP part of the project has also involved laboratory measurements of fundamental properties of SP for CO<sub>2</sub> injection into sedimentary rocks.

In order to compare spatial resolution of seismic, gravity and electromagnetic techniques being considered for CO<sub>2</sub> sequestration monitoring we have used three-dimensional flow simulation models of reservoirs in conjunction with rock-properties relations developed from log data to produce geophysical models from the flow simulations. The model used in this report is based on the proposed Schrader Bluff CO<sub>2</sub> sequestration project on the North Slope of Alaska. The Schrader Bluff reservoir is 30 m thick oil saturated sandstone unit at the depth of 1100 – 1200 m.

The magnitude of the surface gravity response calculated for Schrader Bluff is approximately an order of magnitude above the gravimeter sensitivity, and therefore measurable in the field. However, the difference caused by CO<sub>2</sub> injection over a 5-year period is only about 0.5  $\mu$ Gal, which is in the noise level of the field survey (Hare, 1999). The decrease in the gravitational attraction of the reservoir is caused by increased CO<sub>2</sub> saturations reducing the bulk density of the reservoir. The spatial pattern of the change in the vertical gradient of gravity has a strong correlation with the change in reservoir pressure. Just as with the vertical component of gravity, the magnitude of the gradient signal measured in the field is above the gradiometer accuracy, but the difference between initial conditions and 5 years into CO<sub>2</sub> injection is very small. If the changes in  $dG_z/dz$  could be measured, due to advances in technology, it offers a potential tool for monitoring. In addition to surface gravity measurements, we have also modeled borehole gravity measurements. The difference in both the borehole vertical component of gravity and the borehole vertical gravity gradient ( $dG_z/dz$ ) identifies the position of the reservoir. The sign of the change reflects the changes in the local densities caused by either water or CO<sub>2</sub> saturation changes.

The seismic amplitude associated with the reservoir interval in the Schrader Bluff model shows a large response to changes in water and CO<sub>2</sub> saturation produced by the simulated CO<sub>2</sub> sequestration. In addition, the AVO response of the reservoir reflections shows a significant change as sequestration proceeds. Both amplitude and AVO can be exploited to make quantitative estimates of saturation changes. Forward calculations using Zoeppritz equation for both 2005 and 2020 models support this argument. We have developed an AVO inversion technique for estimating saturations from AVO data that will be applied to the synthetic data set by the end of the project.

The SP method has the potential to be a low-cost low-resolution method of large scale reservoir monitoring. Compared to other geophysical techniques relatively little quantitative work has been done on the SP technique. To quantify the magnitude of the SP response caused by CO<sub>2</sub> injection considerable effort has gone into laboratory measurements of the SP as function of CO<sub>2</sub> injection into sandstone. These studies have shown that the coupling coefficients for CO<sub>2</sub> are large enough to cause an SP signal that could be measured in the field depending on the injection rate, depth of the reservoir and geologic setting. As the CO<sub>2</sub> displaces the water the coupling coefficient decreases. On average, the coupling coefficients observed for CO<sub>2</sub> flow is about 10 times lower than for water flow in the same sample. However, the maximum SP signal comes from the flood front where CO<sub>2</sub>-water mixing is occurring. This provides a benefit in that the signal source region is spatially confined to the advancing front, allowing higher spatial resolution.

## 2.4.2.2 Table of Contents

2.4.2.1 Abstract.....	981
2.4.2.2 Table of Contents .....	982
2.4.2.3 List(s) of Graphical Materials .....	983
2.4.2.4 Introduction.....	985
2.4.2.5 Executive Summary.....	986
2.4.2.6 Experimental.....	988
2.4.2.6.1 Gravity modeling.....	988
2.4.2.6.2 Seismic modeling:.....	996
2.4.2.6.3 Laboratory studies .....	1003
2.4.2.7 Results and Discussion.....	1006
2.4.2.8 Conclusion.....	1007
2.4.2.9 References .....	1008
2.4.2.10 Publications .....	1009
2.4.2.13 Appendix A:.....	1010

### 2.4.2.3 List(s) of Graphical Materials

<b>Figure 1:</b> Three-Dimensional View Of The Portion Of The Reservoir Under Consideration For CO <sub>2</sub> Sequestration Test At Schrader Bluff. Depths Range Between 3800 And 4400 Feet True Vertical Depth.	988
<b>Figure 2a:</b> Cross-Section Of A Density Field (Kg/M <sup>3</sup> ) As A Function Of Depth And Distance In X-Direction.	989
<b>Figure 2b:</b> Plan View Of A Density (Kg/M <sup>3</sup> ) Field At A Depth Z = 1200 M.	989
<b>Figure 3a:</b> Plan View Of A Difference In Model Density (Kg/M <sup>3</sup> ) Between Initial Condition And 5 Years Into CO <sub>2</sub> Injection (Density At 5 Years – Initial Density).	990
<b>Figure 3b:</b> Plan View Of A Difference In Model CO <sub>2</sub> Saturation Between Initial Condition And 5 Years Into CO <sub>2</sub> Injection.	990
<b>Figure 3c:</b> Plan View Of A Difference In Reservoir Pore Pressure (Mpa) Between Initial Condition And 5 Years Into CO <sub>2</sub> Injection.	991
<b>Figure 4a:</b> Difference In The Surface Gravity Response (μGal) Between Initial Conditions And 5 Years Into CO <sub>2</sub> Injection.	991
<b>Figure 4b:</b> Difference In The Vertical Gradient Dg <sub>z</sub> /Dz Response (EU) Between Initial Conditions And 5 Years CO <sub>2</sub> Injection.	992
<b>Figure 5a:</b> Difference In The Gravity Response (μGal) At The Depth Of 1200 M Between Initial Conditions And 20 Years Into CO <sub>2</sub> Injection.	992
<b>Figure 5b:</b> Difference In The Vertical Gradient Dg <sub>z</sub> /Dz Response (EU) At The Depth Of 1200 M Between Initial Conditions And 20 Years CO <sub>2</sub> Injection.	993
<b>Figure 6:</b> Difference In Water Saturation Between 2020 And Initial Conditions. Greens And Blues Are An Increase In Water Saturation, Yellows And Reds Are A Decrease.	993
<b>Figure 7:</b> Difference In CO <sub>2</sub> Saturation Between 2020 And Initial Conditions. Greens And Blues Are An Increase In CO <sub>2</sub> Saturation, Yellows And Reds Are A Decrease.	994
<b>Figure 8:</b> Borehole Gravity Response For Initial Conditions (Blue) And 2020 (Red).	994
<b>Figure 9:</b> Difference Between Gravity Response In 2020 And Initial Conditions.	994
<b>Figure 10:</b> Borehole Vertical Gradient Response (Dg <sub>z</sub> /Dz) For Initial Conditions (Blue) And 2020 (Red).	995
<b>Figure 11:</b> Difference Between Vertical Gradient Response (Dg <sub>z</sub> /Dz) In 2020 And Initial Conditions.	995
<b>Figure 12:</b> Difference In The Acoustic Velocity (Vp) Between 2020 And 2005 Along A 2D Profile Extracted Form The 3D Model Volume. The Profile Runs N45E Across The 3D Model. Note The Significant Decrease In Acoustic Velocity Associated With The Increase In CO <sub>2</sub> Saturation (Figure 13).	996
<b>Figure 13:</b> Difference In The CO <sub>2</sub> Saturation Between 2020 And 2005.	996
<b>Figure 14:</b> Difference In The Water Saturation Between 2020 And 2005.	997
<b>Figure 15:</b> Seismic Response (Shot Gather) For 2005 And 2020.	997
<b>Figure 16:</b> Difference In Seismic Response (Shot Gather) Between 2020 And 2005. Note Amplitude Change And AVO Effects Associated With Water And CO <sub>2</sub> Saturation Changes In The Reservoir.	997
<b>Figure 17a:</b> Velocity Field As A Function Of X Along The Profile (M) And Time (Ms) For 2005.	998
<b>Figure 17b:</b> Velocity Field As A Function Of X Along The Profile (M) And Time (Ms) For 2020.	998
<b>Figure 18a:</b> Stacked Time Section For 2005.	999
<b>Figure 18b:</b> Stacked Time Section For 2020.	999
<b>Figure 19:</b> Angle Stacked Section For 2005 And 2020.	1000
<b>Figure 20:</b> Difference In Stack Section Between 2020 And 2005 (2020-2005).	1000
<b>Figure 21:</b> Workflow For Seismic Synthetic Modeling	1001
<b>Figure 22:</b> Difference In Vp, Vs, And Density Profiles Between 2005 And 2020 For The Schrader Bluff Model At The Center Of Maximum CO <sub>2</sub> Saturation Increase.	1001

<b>Figure 23:</b> Synthetic Gather For 2005 (Scaled To Peak Maximum).	1002
<b>Figure 24:</b> Synthetic Gather For 2020 (Scaled To Peak Maximum).	1002
<b>Figure 25:</b> Difference Between 2020 And 2005 Gathers.	1003
<b>Figure 26:</b> Testing Device Containing Berea Sandstone Core. Sample Is 127 Mm Long And 25 Mm Diameter.	1003
<b>Figure 27:</b> Streaming Potential And Pressure Drop As A Function Of Time As CO <sub>2</sub> Is Injected Into The Core Sample.	1004
<b>Figure 28:</b> Results For Static Head Testing To Determine Water-Only Coupling Coefficient Both Prior To And Following CO <sub>2</sub> Injection Test 2. Resistivity Of Pore Fluid Was 125 Ohm-M. Slope Of Line Indicates Coupling Coefficients Of 20 Mv/0.1mpa (Pre) And 30 Mv/0.1mpa (Post).	1004
<b>Figure 29:</b> Coupling Coefficients As A Function Of Time For The First 20 Minutes Of CO <sub>2</sub> Injection For Samples 1 And 2. Coupling Coefficient Values Were Steady For Times Greater Than 700 Seconds, And Remained Steady Throughout The Remaining Testing Time.	1005
<b>Table 1:</b> Summary Of Coupling Coefficient Results. All Units Are In Mv/0.1mpa.	1005

## 2.4.2.4 Introduction

Cost effective monitoring of reservoir fluid movement during CO<sub>2</sub> sequestration is a necessary part of a practical geologic sequestration strategy. Current petroleum industry seismic techniques are well developed for monitoring production in petroleum reservoirs. The cost of time-lapse seismic monitoring can be born because the cost to benefit ratio is small in the production of profit making hydrocarbon. However, the cost of seismic monitoring techniques is more difficult to justify in an environment of sequestration where the process produces no direct profit. For this reasons other geophysical techniques, which might provide sufficient monitoring resolution at a significantly lower cost, need to be considered.

In order to evaluate alternative geophysical monitoring techniques we have undertaken a series of numerical simulations of CO<sub>2</sub> sequestration scenarios. These scenarios have included existing projects (Sleipner in the North Sea), future planned projects (GeoSeq Liberty test in South Texas) as well as hypothetical models base on generic geologic settings potentially attractive for CO<sub>2</sub> sequestration. In addition, we have done considerable work on geophysical monitoring of CO<sub>2</sub> injection into existing oil and gas fields, including a model study of the Weyburn CO<sub>2</sub> project in Canada and the Chevron Lost Hills CO<sub>2</sub> pilot in Southern California. A paper to be published in September 2003 in Geophysics on the quantitative estimation of CO<sub>2</sub> saturations is included as Appendix A.

Work in 2003 has concentrated in 2 areas; 1) developing a detailed three dimensional numerical model of the proposed Schrader Bluff CO<sub>2</sub> pilot on the North Slope of Alaska and 2) laboratory measurements of the streaming potentials produced by CO<sub>2</sub> injection into brine saturated sedimentary rocks.

Although we are specifically interested in considering “novel” geophysical techniques for monitoring we have chosen to include more traditional seismic techniques as a bench mark so that any quantitative results derived for non-seismic techniques can be directly compared to the industry standard seismic results. This approach will put all of our finding for “novel” techniques in the context of the seismic method and allow a quantitative analysis of the cost/benefit ratios of the newly considered methods compared to the traditional, more expensive, seismic technique.

The Schrader Bluff model was chosen as a numerical test bed for quantitative comparison of the spatial resolution of various geophysical techniques being considered for CO<sub>2</sub> sequestration monitoring. We began with a three dimensional flow simulation model provided by BP Alaska of the reservoir and developed a detailed rock-properties model from log data that provides the link between the reservoir parameters (porosity, pressure, saturations, etc.) and the geophysical parameters (velocity, density, electrical resistivity). The rock properties model was used to produce geophysical models from the flow simulations.

So far we have results from gravity and seismic modeling and laboratory measurements of CO<sub>2</sub> induced streaming potentials in sandstone. Laboratory studies have shown that the streaming potential signal caused by CO<sub>2</sub> injection should be measurable in the field for certain scenarios. This is an interim report, with work on surface seismic, AVO analysis and electromagnetic modeling on-going.

## 2.4.2.5 Executive Summary

Work in 2003 has concentrated in 2 areas; 1) developing a detailed three dimensional numerical model of the proposed Schrader Bluff CO<sub>2</sub> pilot on the North Slope of Alaska and 2) laboratory measurements of the streaming potentials produced by CO<sub>2</sub> injection into brine saturated sedimentary rocks.

Although we are specifically interested in considering “novel” geophysical techniques for monitoring we have chosen to include more traditional seismic techniques as a bench mark so that any quantitative results derived for non-seismic techniques can be directly compared to the industry standard seismic results. This approach will put all of our finding for “novel” techniques in the context of the seismic method and allow a quantitative analysis of the cost/benefit ratios of the newly considered methods compared to the traditional, more expensive, seismic technique.

The Schrader Bluff model was chosen as a numerical test bed for quantitative comparison of the spatial resolution of various geophysical techniques being considered for CO<sub>2</sub> sequestration monitoring. We began with a three dimensional flow simulation model provided by BP Alaska of the reservoir and developed a detailed rock-properties model from log data that provides the link between the reservoir parameters (porosity, pressure, saturations, etc.) and the geophysical parameters (velocity, density, electrical resistivity). The rock properties model was used to produce geophysical models from the flow simulations.

So far we have results from gravity and seismic modeling and laboratory measurements of CO<sub>2</sub> induced streaming potentials in sandstone. Laboratory studies have shown that the streaming potential signal caused by CO<sub>2</sub> injection should be measurable in the field for certain scenarios. This is an interim report, with work on surface seismic, AVO analysis and electromagnetic modeling on-going.

The magnitude of the surface gravity response over the Schrader Bluff model (3 mGal) is about an order of magnitude above the gravimeter sensitivity, and therefore measurable in the field, the difference caused by CO<sub>2</sub> injection for a period of five years is only about 0.5 μGal, which is in the noise level of the field survey (Hare, 1999). The reduction in the vertical component of gravity is caused by increased CO<sub>2</sub> saturations reducing the bulk density of the reservoir. The change in the vertical gradient of gravity has a strong correlation with the change in pressure within the reservoir. Again, the magnitude of the signal which would be measurable in the field (2–10 EU) is above the gradiometer accuracy (0.5–1 EU), but the difference between initial conditions and 5 years into CO<sub>2</sub> injection is very small (~0.005 EU). This change in vertical gradient would be considered undetectable given current estimates of gradiometer accuracy. However, if the changes in  $dG_z/dz$  could be measured, due to advances in technology, measurement procedures and background noise reduction, the model results show a high degree of spatial correlation between changes in  $dG_z/dz$  and the pressure changes, offering a potential low cost monitoring tool.

The time-lapse changes in the borehole gravity response and in the vertical gravity gradient ( $dG_z/dz$ ) clearly identifies the position of the reservoir. The sign of the change reflects the changes in the local densities caused by either water or CO<sub>2</sub>.

There is a significant change in seismic amplitude associated with the reservoir caused by the changes in water and CO<sub>2</sub> saturation as sequestration proceeds. In addition, there is a large change in the AVO response from the reservoir interval. Both seismic amplitude and AVO can be exploited to make quantitative estimates of saturation changes. Forward calculations using Zoeppritz equation for both five and twenty years into injection support this argument. We have developed an AVO inversion technique for estimating saturations from AVO data that will be applied to the synthetic data set in by the end of the project.

Laboratory studies showed that the coupling coefficients for CO<sub>2</sub> are large enough to cause SP signal measurable in the field. As the CO<sub>2</sub> displaces the water the coupling coefficient decreases. On average, the coupling coefficients observed for CO<sub>2</sub> flow is about 10 times lower than for fresh water flow in the same sample. The most effective way to spatially monitor injected CO<sub>2</sub> flow is to monitor the progressing CO<sub>2</sub>/water front, where the coupling coefficient is largest.

### 2.4.2.6 Experimental

In order to compare spatial resolution of various geophysical techniques being considered for CO<sub>2</sub> sequestration monitoring we have used a three-dimensional flow simulation model of reservoirs in conjunction with rock-properties relations developed from log data to produce geophysical models from the flow simulations. Work in this report is done for the model based on the proposed Schrader Bluff CO<sub>2</sub> sequestration project on the North Slope of Alaska. The Schrader Bluff reservoir is 30 m thick sandstone unit at the depth of 1100 – 1200 m. . Figure 1 shows a 3-D view of the portion of the reservoir under consideration for a CO<sub>2</sub> sequestration test.

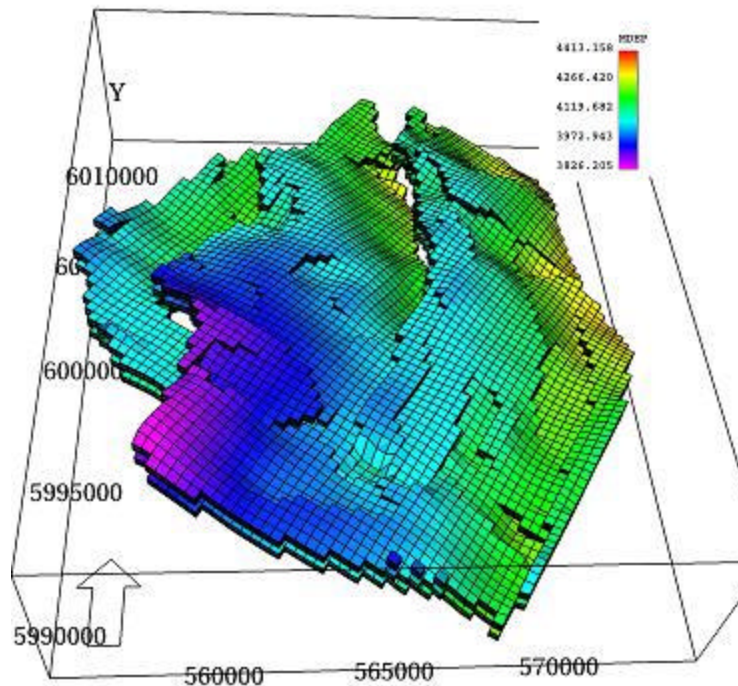


Figure 1: **Three-dimensional view of the portion of the reservoir under consideration for CO<sub>2</sub> sequestration test at Schrader Bluff. Depths range between 3800 and 4400 feet true vertical depth.**

Rock properties models were developed from log data for the reservoir. These models relate reservoir parameters to geophysical parameters and are used to convert the flow simulation models to geophysical models ( $V_p$ ,  $V_s$ , density and electrical resistivity). A detailed description of the rock-properties modeling process is given by Hoversten et al. 2003. Time-lapse snapshots of the reservoir at initial conditions and 5-year increments out to 2035 were used. The injection strategy is to inject alternating slugs of water and CO<sub>2</sub> (WAG). This produces complicated spatial variations in both CO<sub>2</sub> and water saturation within the reservoir over time.

#### 2.4.2.6.1 Gravity modeling

A snapshot of the model at initial conditions, before CO<sub>2</sub> injection begins, is shown in Figure 2. Figure 2a is a cross-section of bulk density as a function of depth and distance in the x-direction between a pair of injection wells. The reservoir interval is outlined in white on Figure 2a. Figure 2b is a plan view of the density at initial conditions at a depth of 1200 m. The positions of the gravimeters are indicated by black squares. In this case, Figure 2a shows gravimeters located in two wells roughly 8 km apart. Spacing between the gravimeters in depth ( $z$ ) is 10 m outside of the reservoir and 5 m inside of the reservoir. The plan view of the reservoir (Figure 2b) shows positions of 23 injecting wells taken from the reservoir simulation.

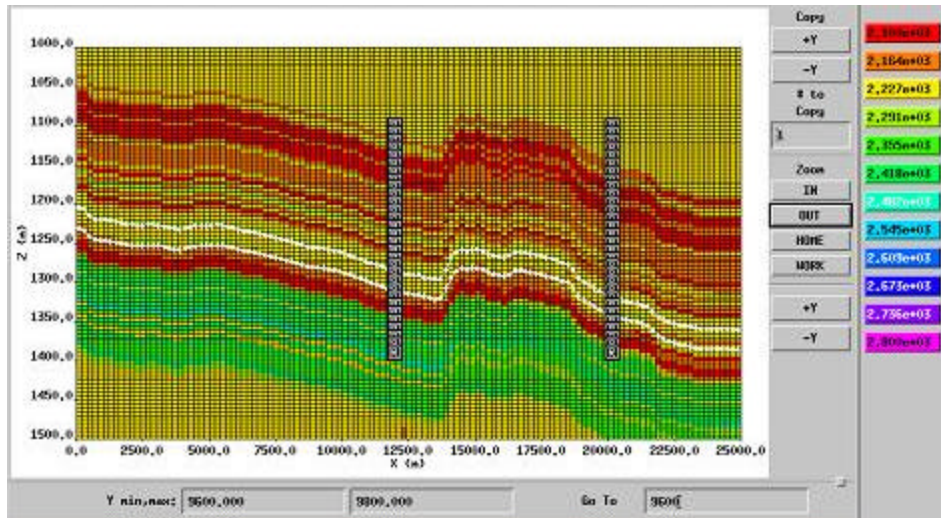


Figure 2a: Cross-section of a density field ( $\text{kg/m}^3$ ) as a function of depth and distance in x-direction.

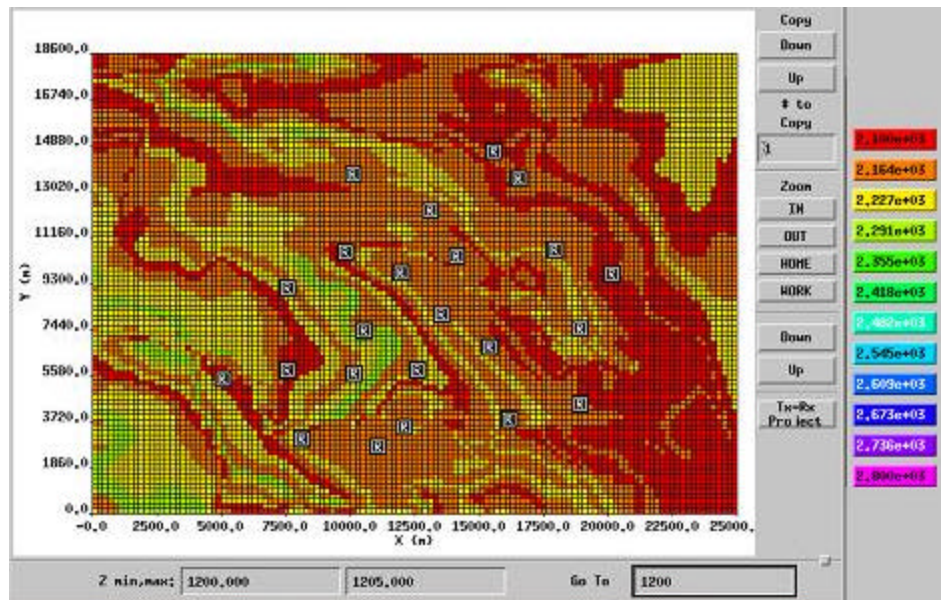


Figure 2b: Plan view of a density ( $\text{kg/m}^3$ ) field at a depth  $z = 1200$  m.

Figure 3 shows a plan view of differences in the model density,  $\text{CO}_2$  saturation, and reservoir pore pressure, respectively, between initial conditions and 5 years into  $\text{CO}_2$  injection.

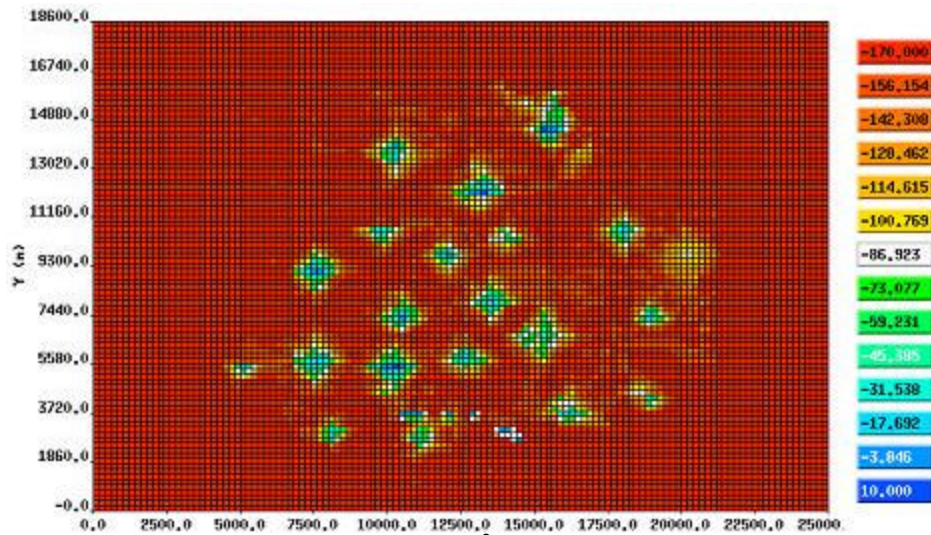


Figure 3a: Plan view of a difference in model density ( $\text{kg/m}^3$ ) between initial condition and 5 years into  $\text{CO}_2$  injection (density at 5 years – initial density).

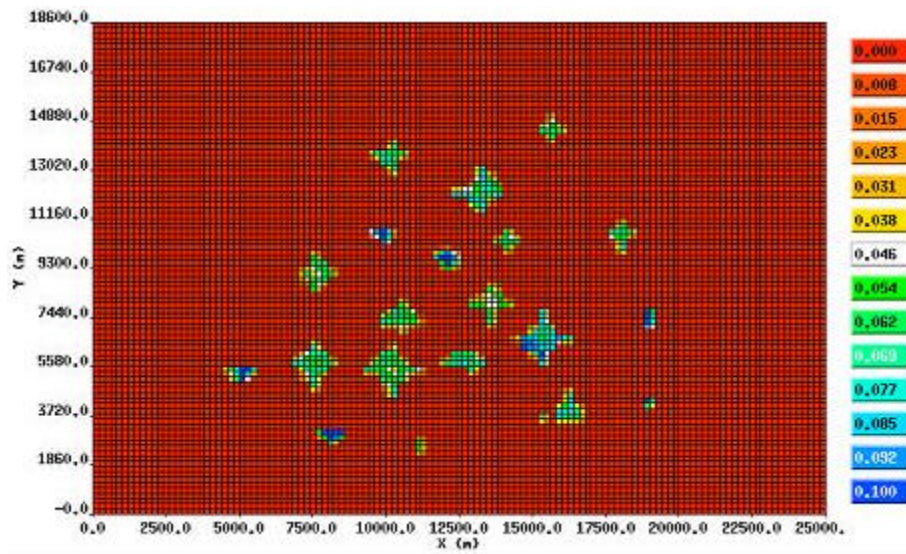


Figure 3b: Plan view of a difference in model  $\text{CO}_2$  saturation between initial condition and 5 years into  $\text{CO}_2$  injection.

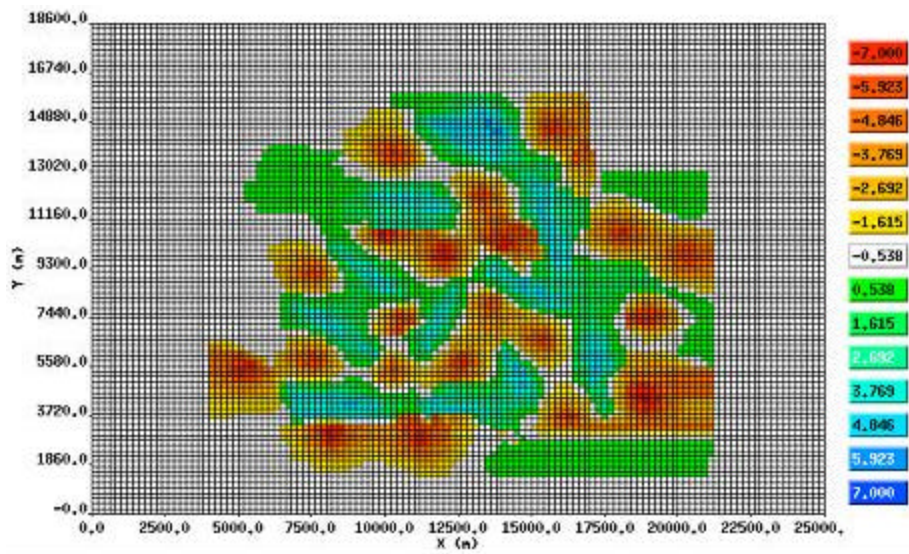


Figure 3c: Plan view of a difference in reservoir pore pressure (MPa) between initial condition and 5 years into CO<sub>2</sub> injection.

Surface and borehole gravity responses have been calculated for this model. The surface gravity response was calculated for a grid of stations with 1 km spacing from 2000 m to 22000 m in x and from 2000 m to 16000 m in y direction. Figure 4a shows a difference in the surface gravity response between initial conditions and 5 years into CO<sub>2</sub> injection. Although the magnitude of the surface vertical component of gravity (3 mGal) is about an order of magnitude above the gravimeter sensitivity, and therefore measurable in the field, the difference caused by CO<sub>2</sub> injection is only about 0.5  $\mu$ Gal, which is in the noise level of the field survey (Hare, 1999). The decrease in the vertical component of gravity is caused by increased CO<sub>2</sub> saturations reducing the bulk density of the reservoir.

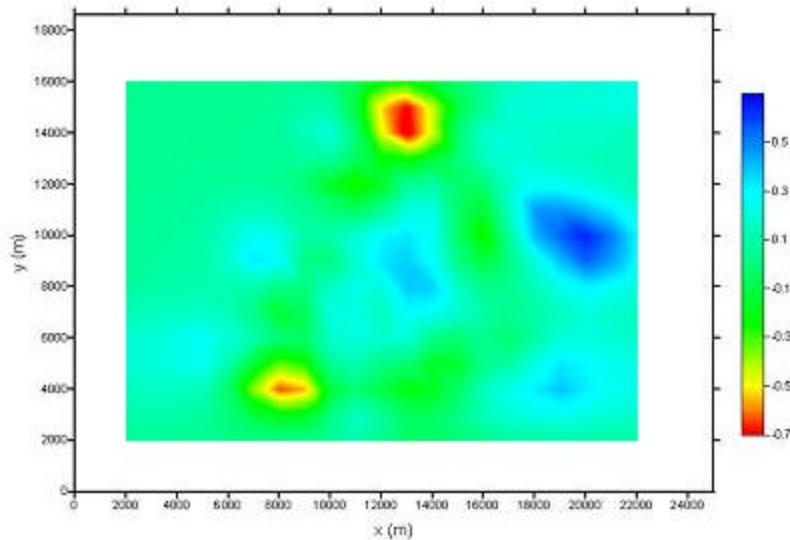


Figure 4a: Difference in the surface gravity response (mGal) between initial conditions and 5 years into CO<sub>2</sub> injection.

*The change in the vertical gradient of gravity (Figure 4b) has a strong correlation with the change in the reservoir pressure. Again, the magnitude of the signal measured in the field (2–10 EU) is above the gradiometer accuracy (0.5–1 EU), but the difference between initial conditions and 5 years into CO<sub>2</sub> injection is very small (~0.005 EU). If the relationship between pressure changes in the reservoir and the changes in  $dG_z/dz$  could be measured by future technology, it offers an obvious tool for monitoring. These results suggest future analysis to determine the maximum sensitivity of  $dG_z/dz$  that*

could be obtained by permanent emplacement of sensors with continuous monitoring coupled with real-time data reduction to reduce noise levels.

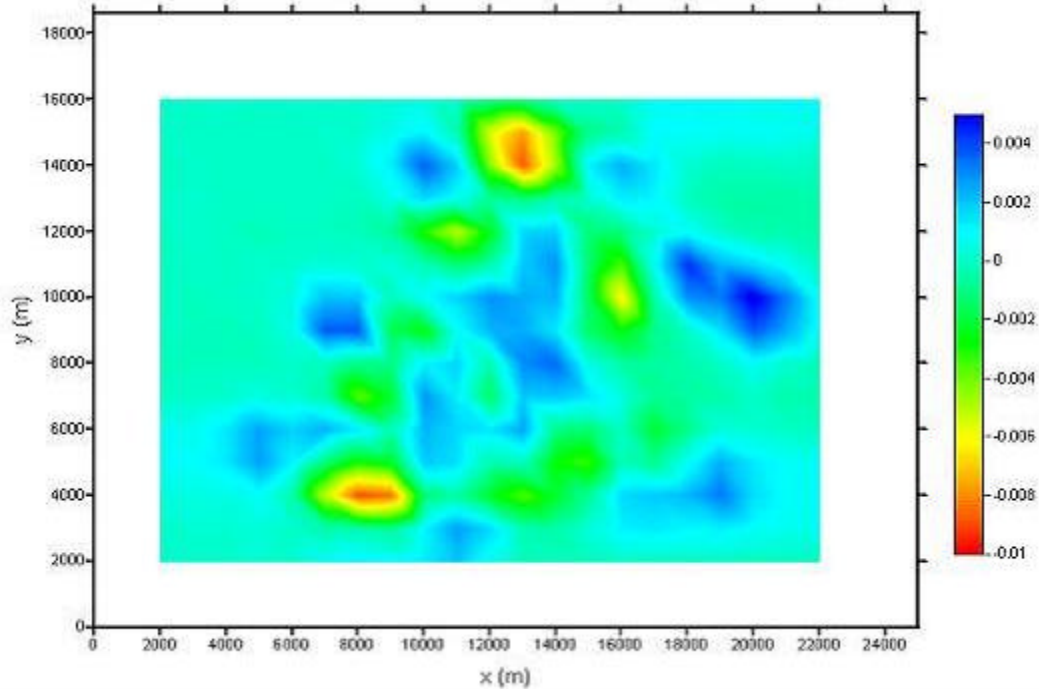


Figure 4b: Difference in the vertical gradient  $dG_z/dz$  response (EU) between initial conditions and 5 years  $\text{CO}_2$  injection.

Similar plots done for initial condition and 20 years into  $\text{CO}_2$  injection at the depth of 1200 m are shown in Figure 5. Figure 5a is a difference in the gravity response, while Figure 5b is a difference in the vertical gradient response. The magnitude of the differences in both plots increased, although only the difference in the gravity response would be measurable in the field.

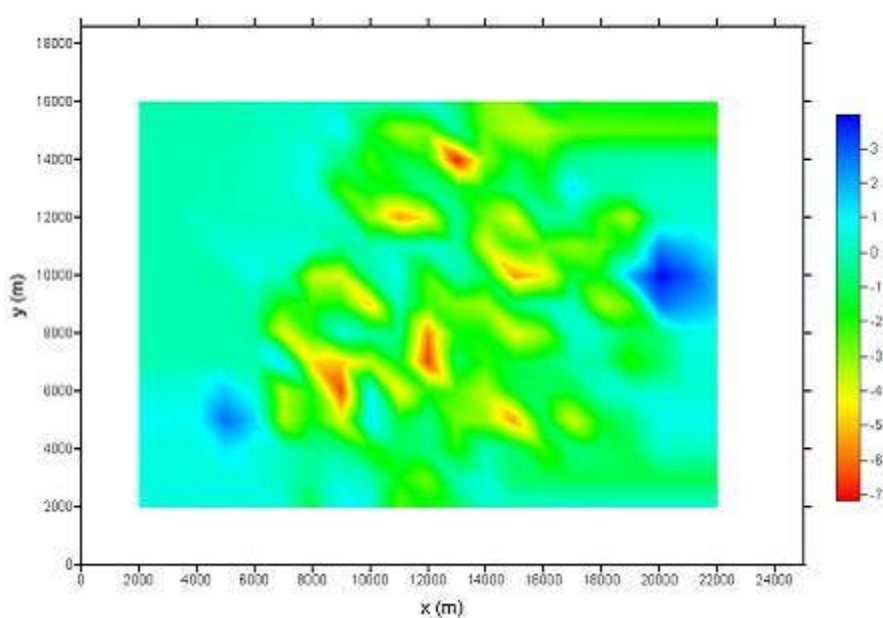


Figure 5a: Difference in the gravity response (mGal) at the depth of 1200 m between initial conditions and 20 years into  $\text{CO}_2$  injection.

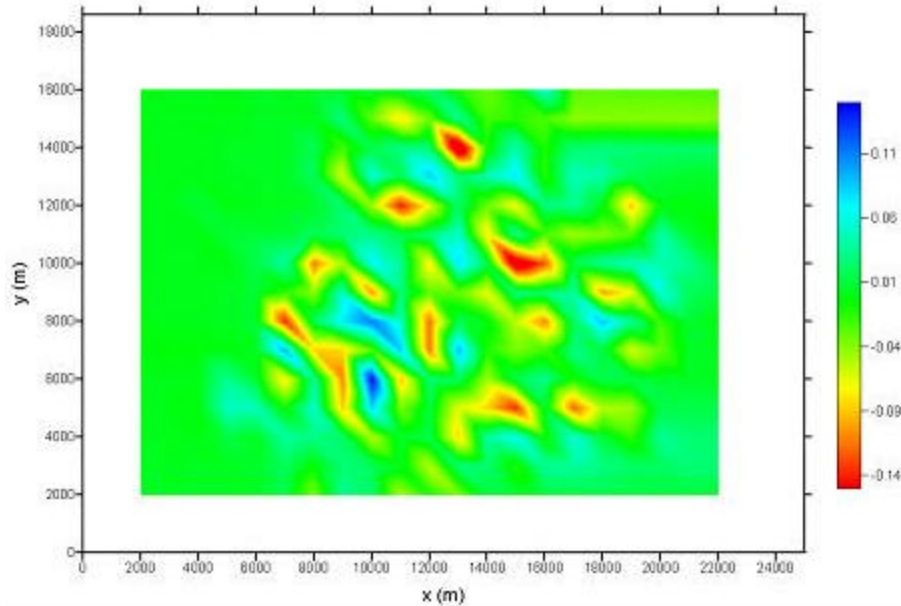


Figure 5b: Difference in the vertical gradient  $dG_z/dz$  response (EU) at the depth of 1200 m between initial conditions and 20 years  $CO_2$  injection.

In addition to surface gravity and gravity gradient responses we have analyzed borehole gravity as well. Figure 6 is the difference in the water saturation between 2020 and initial conditions along a vertical slice through the reservoir at an injection well. Figure 7 is the difference in the  $CO_2$  saturation between 2020 and initial conditions. At the top of the reservoir near the injection well, the water saturation decreases while the  $CO_2$  saturation increases. At the bottom of the reservoir, there is no  $CO_2$  while the water saturation increases due to migration of water away from the injected  $CO_2$ . The vertical component of gravity measured in the borehole, shown in Figure 8, reflects this change by a decrease in the response at the top of the reservoir, and an increase in the response at the bottom of the reservoir. The change in the response is  $\pm 8 \mu\text{Gal}$ . The reservoir is between 1325 and 1350 m. The difference in gravity response between 2020 and initial conditions (Figure 9) identifies the position of the reservoir. The sign of the change reflects the changes in the local densities caused by either water or  $CO_2$ . In both figures, Figure 8 and 9, the reservoir is outlined by the blue area.

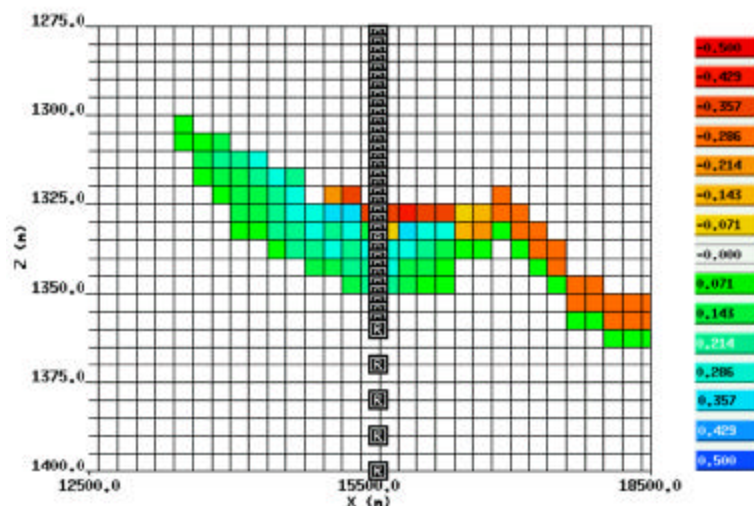


Figure 6: Difference in water saturation between 2020 and initial conditions. Greens and blues are an increase in water saturation, yellows and reds are a decrease.

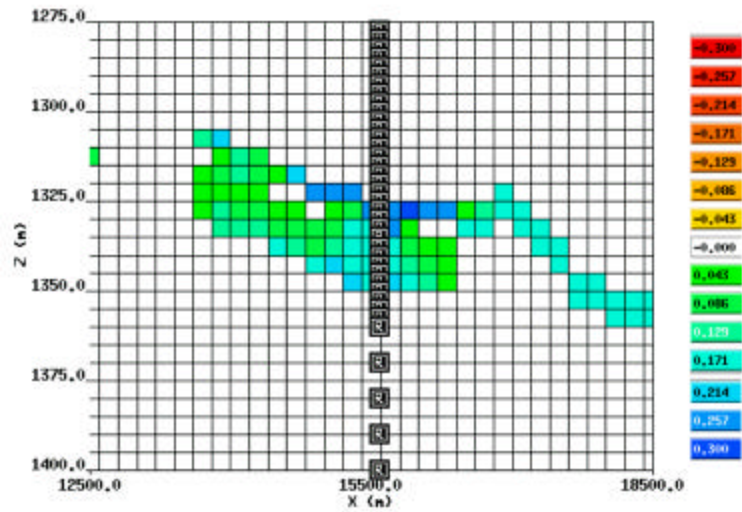


Figure 7: Difference in CO<sub>2</sub> saturation between 2020 and initial conditions. Greens and blues are an increase in CO<sub>2</sub> saturation, yellows and reds are a decrease.

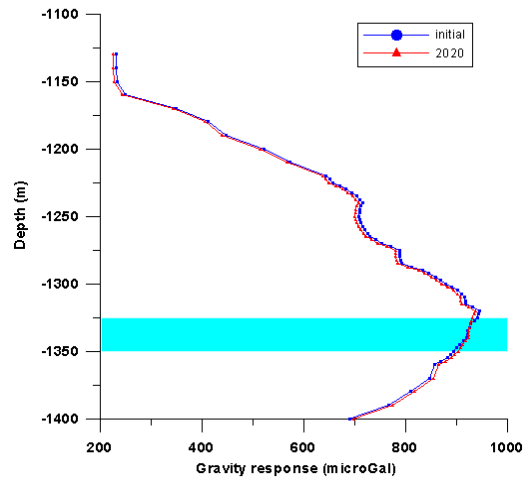


Figure 8: Borehole gravity response for initial conditions (blue) and 2020 (red).

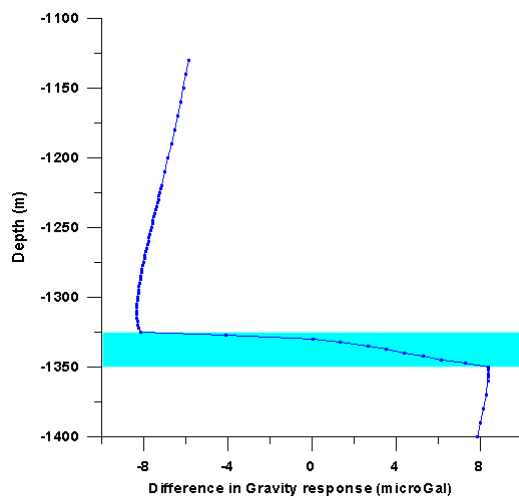


Figure 9: Difference between gravity response in 2020 and initial conditions.